Molecular Crystals and Liquid Crystals
Publication details, including instructions for authors and subscription information:
http://www.tandfonline.com/loi/gmcl20

Biomineralization Processes in Formation of Urolits

Ion Iosub [a], Viorel Malinovschi [a], Florin Miculescu [b] & Aurelia Meghea [b]

[a] Faculty of Science, University of Pitesti, Pitesti, Romania

[b] University POLITEHNICA of Bucharest, Romania, Bucharest

Version of record first published: 28 May 2010

To cite this article: Ion Iosub, Viorel Malinovschi, Florin Miculescu & Aurelia Meghea (2010): Biomineralization Processes in Formation of Urolits, Molecular Crystals and Liquid Crystals, 523:1, 139/[711]-147/[719]

To link to this article: http://dx.doi.org/10.1080/15421401003726691

Mol. Cryst. Liq. Cryst., Vol. 523: pp. 139/[711]–147/[719], 2010

ISSN: 1542-1406 print/1563-5287 online
DOI: 10.1080/15421401003726691

Taylor & Francis
Taylor & Francis Group

Biomineralization Processes in Formation of Urolits

ION IOSUB,[1] VIOREL MALINOVSCHI,[1]
FLORIN MICULESCU,[2] AND AURELIA MEGHEA[2]

[1]Faculty of Science, University of Pitesti, Pitesti, Romania
[2]University POLITEHNICA of Bucharest, Romania, Bucharest

Formation of renal calculi can be caused by various dietary disturbances, being influenced by disorders of metabolic conditions such as hypercalcemia (hypertiroidism), hyperoxaluria (dietary, enteric, primary), hypocytruria, hyperuricosuria, etc. In this article, a number of structural parameters of renal calculi with binary composition oxalates – urates have been analysed by adequate techniques: X-ray diffraction, FT-IR spectroscopy, optical microscopy and SEM/EDS. For the biggest urolits a detailed analysis on radial differentiated sections has been performed with the aim to identify the initiator role in nucleation process and to find out the mechanism and the main steps in calculi growth.

Keywords Biomineralization mechanism; renal calculi; structural analysis of urolits

Introduction

Urolits, known as generic term for kidney stones or renal calculi, have a variety of origins of which the most common is calcium oxalate. Their size is ranging from few mm to several cm orders, being frequently found in adults, with higher incidence in men compared to women, and in hot climate compared to cold regions. While calcium intake has always been considered to be responsible for stone formation, new evidences suggests that low calcium levels can have significant contribution as well.

The biomineralization represents the initial process in formation of the bone, teeth, cartilages and kidney stones. In this process the transport is achieved by electric charge properties of different biomolecules: polyelectrolites phosphoproteines, enzymes, calcium ions which are binding phospholipides and proteins. The pathogenesis of kidney stones involve many factors: age, sex, obesity, hypertension and several external environmental that might influence the biomineral formation, as occupation, physical activity, diet, geograpical, location.

Therapy for preventing renal calculi relapse needs a quantitative evaluation of calculi composition and its correlation with other external factors, such as diet, active or sedentary living style, hydration regime, composition of daily water consume, etc. This last correlation has been analyzed by several authors in some

Address correspondence to Aurelia Meghea, University Politehnica of Bucharest, 1 Polizu Street, Bucharest 011061, Romania. Tel.: 0040213154193; Fax: 0040213154193; E-mail: a_meghea@gmail.com

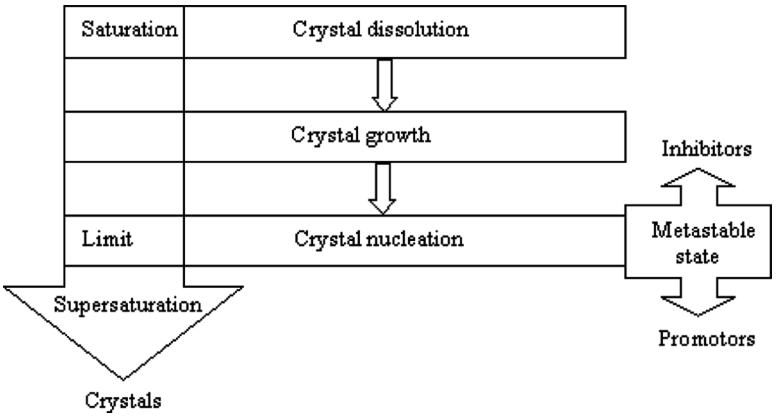

Figure 1. Mechanism of renal calculi formation.

previous papers [1,2], when the constituents of some kidney calculi drawn after surgery from 90 patients have been identified to be related with hard drinking waters existent in the area investigated.

Another interesting aspect that should be taken in consideration is referred to the research on composition of various heterogeneous structures present within studied calculi in order to establish some possible chemical and biochemical steps that could determine their formation [3,4]. Among the main factors responsible for renal calculi formation could be mentioned the following: hypercalcemia (hyperthyroidism), hyperoxalurea, hypocitraturea, and hyperuricosurea. According to the last factor, the relative high content in uric acid in urine could promote the apparition of calculi based on calcium oxalate (CaO_x) in a proportion of 20–35%. In this respect, there are numerous papers that mention the role of urates in (CaO_x) nucleation [2–6], and the steps involved in formation of the first calculi crystals could be modeled based on the mechanism presented in the Figure 1.

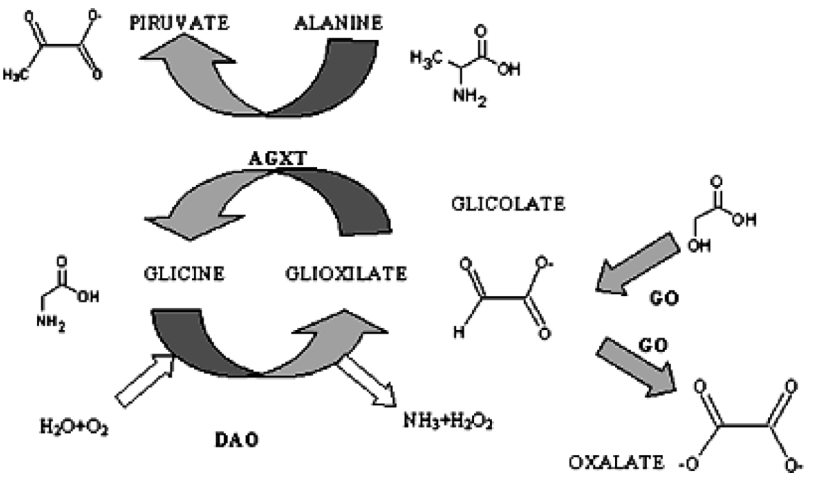

Figure 2. Modeling of metabolic process of oxalate formation in liver.

The process of calculi formation is directed by enzyme activity at the liver level, when metabolic disorders are produced as a result of diminution in concentration of alanineglycoxylate aminotransferase (AGXT). The main contribution of this enzyme consists in the degradation of glycoxylate to the level of peroxysomes, organoids of the cells inside the liver [7]. The other two enzymes involved are: D-amino oxidase (DAO) and glicolate oxidase (GO), as it is illustrated in Figure 2.

In order to bring relevant arguments in supporting these mechanisms, the aim of this article is to do a detailed analysis of structural parameters of some representative sections within a renal calcul, radial differentiated during the growth steps of stone, and thus to identify the species with initiator role in the nucleation process and to elucidate the main steps of calculi evolution.

Experimental

A number of three samples has been collected from three main zones identified to be relevant for the composition evolution during the stone growth, as it is indicated in the Figure 3: 1 – inner zone, dark brown, 2 – median zone, yellow, and 3 – outer zone, brown grey.

Methods for investigation and equipment

- The microphotographs were taken by optical microscop digital INTEL.
- X Ray diffraction has been registered by means of a Rigaku Ultima IV diffractometer, endowed with CBO (Cross Beam Optics) and Bragg Brenteno

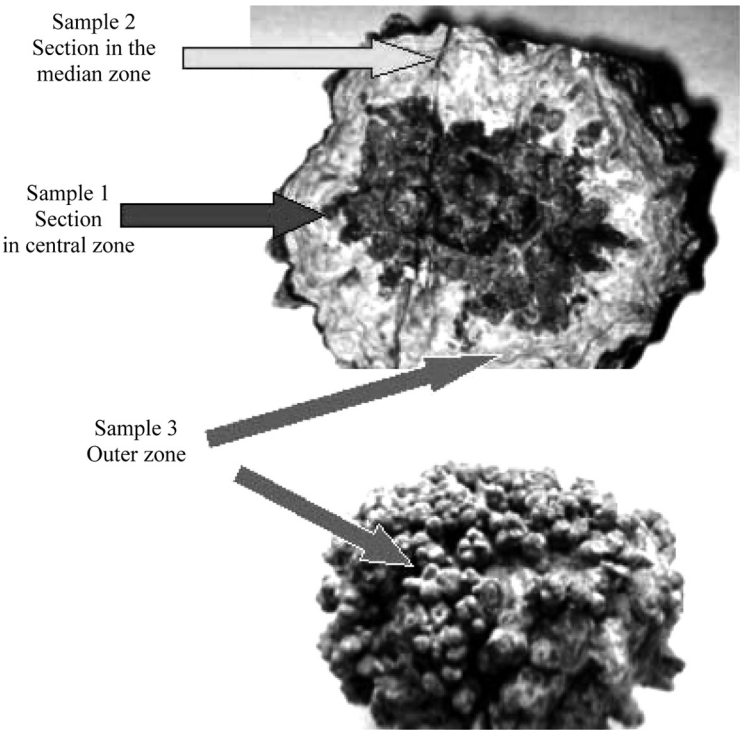

Figure 3. The structure in section of the analyzed urolit.

parallel optics in geometry. The acquisition conditions were the following: The divergent slit of 0.5 mm on the incident fascicle, monocromator made of graphite on the diffracted fascicle, U = 40 KV, I = 30 mA, I = 30 mA, $2\theta = [10°, 70°]$, $\Delta(2\theta) = 0.02°$, $\tau = 5$ s;

- Spectral analysis has been performed in KBr pellets by using an FT-IR 620 (Jasco) spectrometer on the domain 4000–400 cm^{-1}.
- For the compositional qualitative and quantitative analysis an electronic microscope Philips XL 30 ESEM TMP, with 3.5 nm resolution and an acceleration tension of electron beam of 25 kV has been used. The analysis of chemical composition was achieved by an energy dispersive X-ray spectrometer EDS, EDAX – Saphire, with a resolution of 128 eV. The acquisition time of data was established at minimum 25 Lsec and the results have been reported in mass (Wt) and atomic (At) percents.

Results and Discussion

As can be seen in Figure 3, the three samples collected from central, median and external zones are different both in aspect and in their colour, as a result of various mineralogical structures determined by XRD (Fig. 4).

According to XRD measurements, two main components have been identified: urate in uricite, with formula $C_4(NH)_2O_2(NH)_2O$, JCPDS 31-1982, monoclinic, and

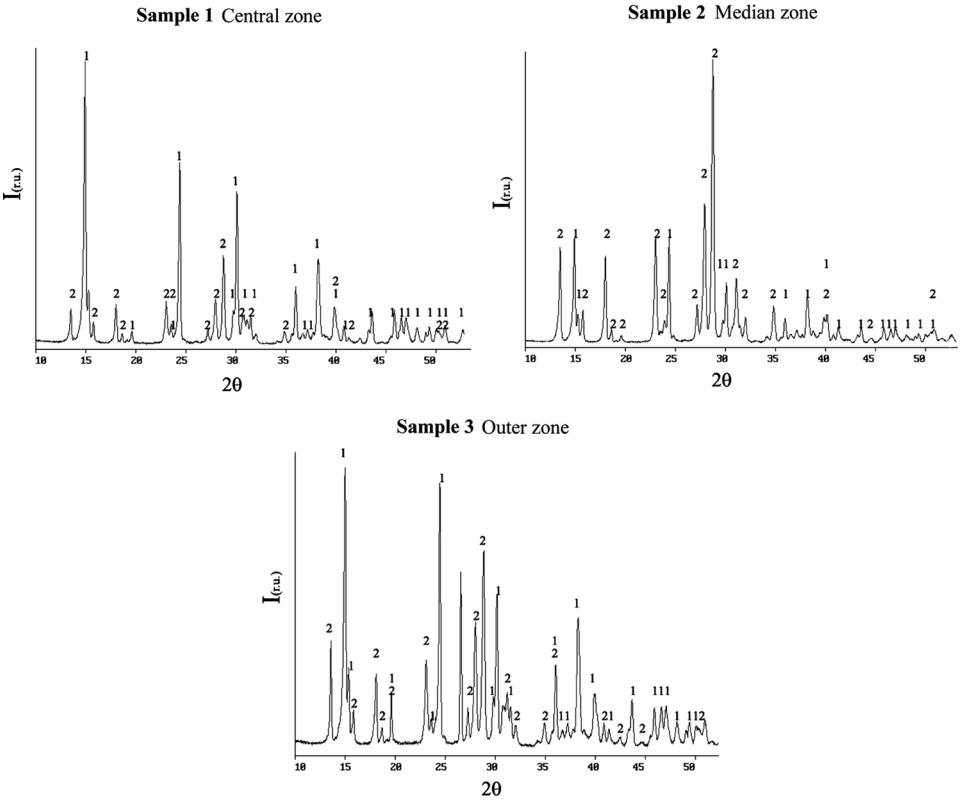

Figure 4. XRD spectra for the investigated zones.

Table 1. Mineralogical composition of the investigated sections

Sample/ zone	Volume concentration, %			Mass concentration, %		
	Uricite	Whewellite	Residue dipeptide	Uricite	Whewellite	Residue dipeptide
1 – inner	73.9	26.1	–	70.2	29.8	–
2 – median	94.4	5.6	–	93.3	6.7	–
3 – outer	76.3	13.4	10,3	76.3	16.1	7,6

calcium oxalate monohydrate, $CaC_2O_4 \cdot H_2O$, JCPDS 20-0231, monoclinic, also known as whewellite.

The proportions of these two components within the main zones differentiated during the development of investigated urolit are presented in the Table 1. It can be noted the preponderance of urate over calcium oxalate, the maximum weight being in the median zone (sample 2). Moreover, in the outer zone (sample 3) the characteristic lines associated with $CH_3(CNOH)_2CH_3$ or $C_4H_8N_2O_2$ phases, JCPDS 26-1836, have been identified, that could be assessed to dipeptide residues.

IR spectra (Fig. 5) confirm these compositions, the main characteristic vibration bands for the samples 1 and 3 being specific to kidney stones with a significant content in calcium oxalate monohydrate. The group of bands in 3000–3500 cm^{-1} is assigned to water stretching vibrations. Other specific bands appear at 1650 cm^{-1} for asymmetric vibration of the COO group of oxalate, 1310 cm^{-1} for symmetric vibration, 770 and 520 cm^{-1} for deformation vibrations of this group [8]. However, for the sample 2, with uricite as major constituent, the IR spectrum is different in the region 2800–3300 cm^{-1}, being characteristic for N-H vibrations of amino groups from urates.

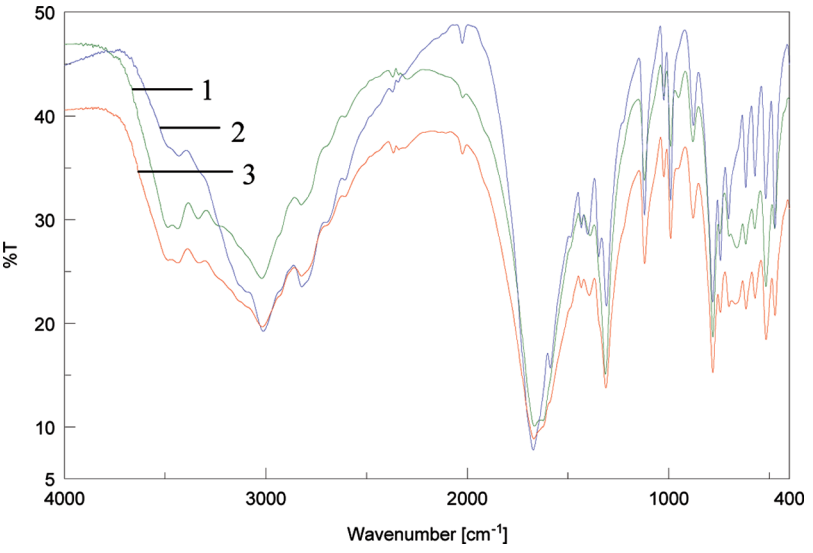

Figure 5. FT-IR spectra for the three samples.

These compositions are also confirmed by SEM/EDS analyses illustrated in the Figures 6–8 for the three zones.

Detailed quantitative compositional analysis performed on light and dark grey regions evidenced on SEM images revealed very different element contents.

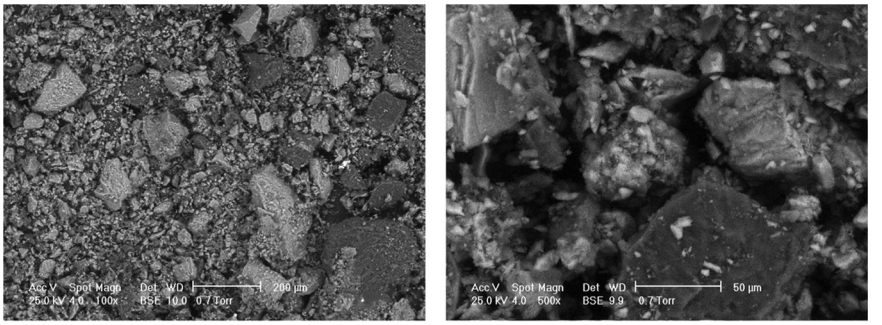

(a) (b)

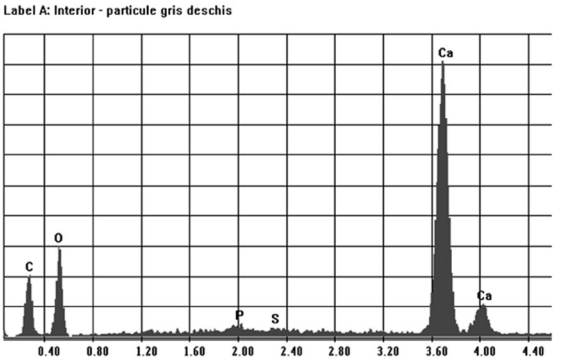

Element	*Wt %*	*At %*
C	*32.38*	*44.35*
O	*45.06*	*46.33*
P	*0.35*	*0.19*
S	*0.21*	*0.11*
Ca	*21.99*	*9.02*
Total	*100.000*	*100.000*

(c)

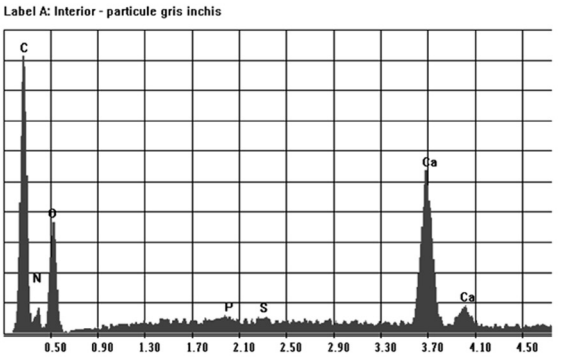

Element	*Wt %*	*At %*
C	*47.27*	*54.66*
N	*19.49*	*19.32*
O	*27.73*	*24.07*
P	*0.18*	*0.08*
S	*0.17*	*0.07*
Ca	*5.17*	*1.79*
Total	*100.000*	*100.000*

(d)

Figure 6. SEM/EDS analysis for sample 1. (a) SEM image for sample 1; (b) Detail on SEM image of sample 1; (c) EDS analysis of light grey particles on SEM image of sample 1, Quantitative compositional analysis corresponding to the spectrum in (c) and (d) EDS analysis of dark grey particles on SEM image of sample 1, Quantitative compositional analysis corresponding to the spectrum in (d).

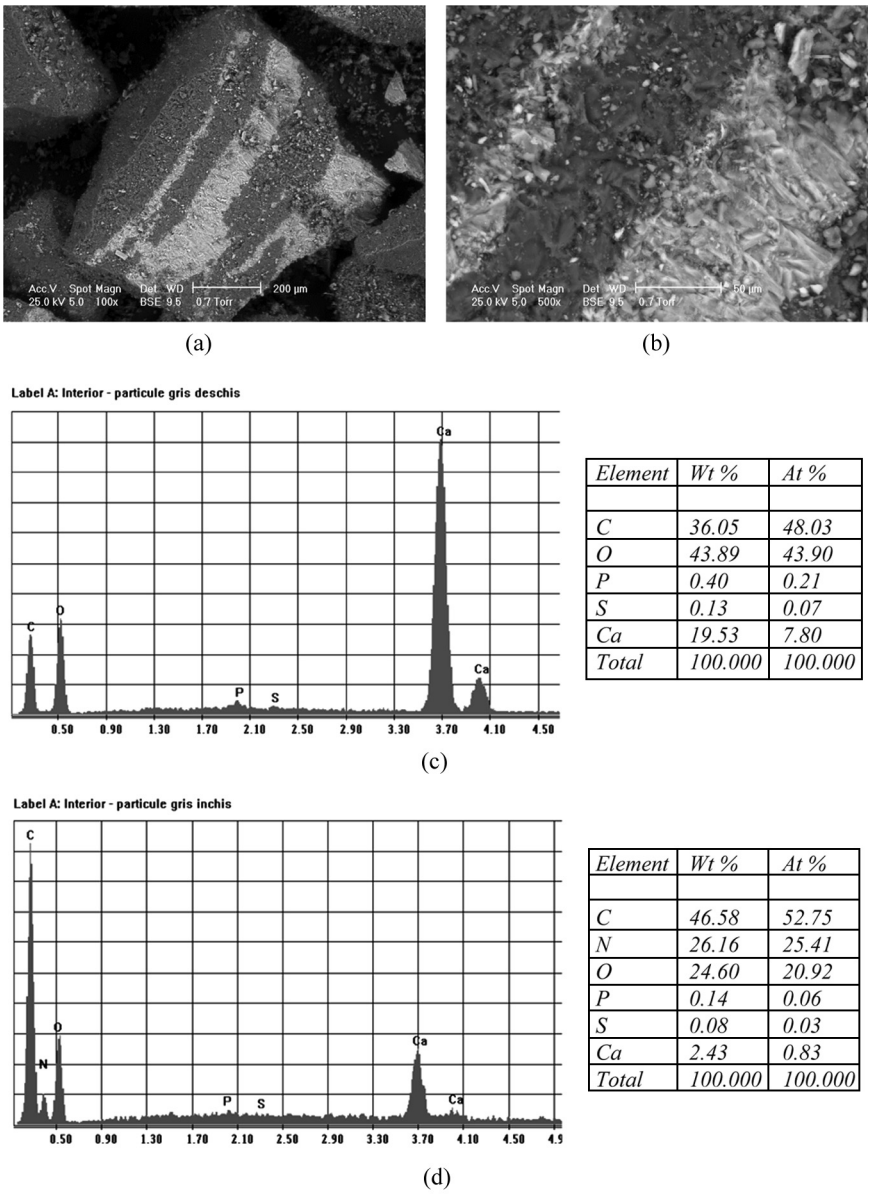

Element	*Wt %*	*At %*
C	*36.05*	*48.03*
O	*43.89*	*43.90*
P	*0.40*	*0.21*
S	*0.13*	*0.07*
Ca	*19.53*	*7.80*
Total	*100.000*	*100.000*

Element	*Wt %*	*At %*
C	*46.58*	*52.75*
N	*26.16*	*25.41*
O	*24.60*	*20.92*
P	*0.14*	*0.06*
S	*0.08*	*0.03*
Ca	*2.43*	*0.83*
Total	*100.000*	*100.000*

Figure 7. SEM/EDS analysis for sample 2. (a) SEM image for sample 2; (b) Detail on SEM image of sample 2; (c) EDS analysis of light grey particles on SEM image of sample 2, Quantitative compositional analysis corresponding to the spectrum in (c) and (d) EDS analysis of dark grey particles on SEM image of sample 2, Quantitative compositional analysis corresponding to the spectrum in (d).

If compare these data with elemental composition calculated for the two constituents (Table 2) a good agreement with XRD data presented in Table 1 could be noticed.

Even though the uricite is the major component present in all three layers analyzed as samples, the higher contents in calcium and oxygen registered on light grey

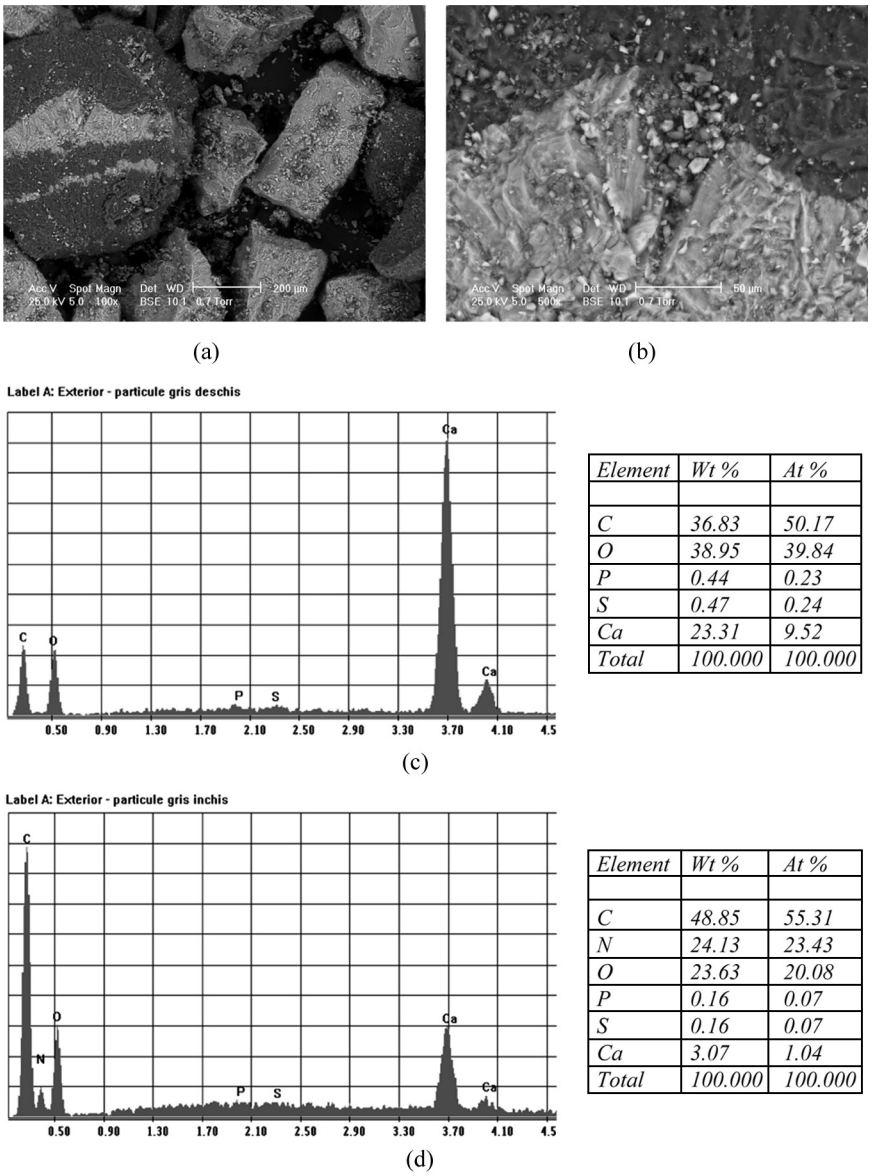

Element	Wt %	At %
C	36.83	50.17
O	38.95	39.84
P	0.44	0.23
S	0.47	0.24
Ca	23.31	9.52
Total	100.000	100.000

Element	Wt %	At %
C	48.85	55.31
N	24.13	23.43
O	23.63	20.08
P	0.16	0.07
S	0.16	0.07
Ca	3.07	1.04
Total	100.000	100.000

Figure 8. SEM/EDS analysis for sample 3. (a) SEM image for sample 3; (b) Detail on SEM image of sample 3; (c) EDS analysis of light grey particles on SEM image of sample 3, Quantitative compositional analysis corresponding to the spectrum in (c) and (d) EDS analysis of dark grey particles on SEM image of sample 3, Quantitative compositional analysis corresponding to the spectrum in (d).

regions suggests the presence of whewellite, while the significant percentage in nitrogen on dark grey regions is a clear proof on the existence of uricite, in a highest proportion for the median zone.

The investigation of the stone shows concentric or radial lamination organised in compact fibrils between concentric substrates. The maximum concentration of

Table 2. Elemental composition of mineralogical constituents

Component	C, %	O, %	H, %	Ca, %	N, %
Whewellite	16.44	54.80	1.36	27.47	–
Uricite	35.71	28.57	2.38	–	33.33
Dipeptide residue	41.37	27.58	6.89	–	24.13

organic material in the sample 3 – outer zone, also revealed by maximum carbon content, is supported by the phases specific to dipeptide residues identified in XRD spectrum (Fig. 4), this suggesting a possible migration, in time, of aminoacid components from the inner to outer areas of the stone. In the Figure 8b is shown a possible coating process of crystals by the organic material.

Even more, the low but still detected contents in phosphorus and sulphur suggests the involvement of some organic biopolymers, such as phospholipids and proteins, possible to be involved during the biomineralization processes of urolits, rather than of inorganic components, like phosphates and sulphates. It follows that formation and evolution of urolits can be influenced not only by the calcium in-take from drinking water, but also by the content in oxalates of diet based on vegetable and dairy products and/or by the amount and quality of meat products consumed in various periods of life, the last type of food being responsible for urate formation.

Conclusion

The compositional changes noticed during the evolution of mineralogical structure of urolits can be successfully followed by corroboration of data provided by adequate instrumental techniques: optical microscopy, XR diffraction, infrared spectroscopy and SEM/EDS analysis.

Chemical and metabolic mechamisms of urolit nucleation and development could be influenced by various external and internal factors related to both the content in calcium in drinking water and the quantity and quality of food responsible for the up-take of oxalates and urates.

This study of such biomineralization processes might be also useful in designing novel synthetic hybrid biomaterials obtained in biomimetic self-organized systems.

References

[1] Pragnya, A. B. & Parimal, P. (2008). *J. Chem. Sci.*, *120*, 267.
[2] Coulter-Makie, M. B. (2006). *Kidney Internat.*, *70*, 1891.
[3] Weston, J. & Ward, M. (2007). *Elements.*, *3*(6), 415.
[4] Khan, S. R. (1995). *Scanning Microscopy*, *9*, 597.
[5] Opalko, F. J., Khan, S. R., & Adair, J. H. (1997). *J Crystal Growth*, *181*, 410.
[6] Sundaramoorthi, P. & Kalainathan, S. (2007). *J Minerals & Materials & Characterization & Enginnering*, *6*(1), 17.
[7] Raju, D. L., Cantarovich, M., Brisson, M. L., Tchervenkov, J., & Lipman, M. L. (2008). *Am J Kidney Dis.*, *51*(1), el–e5.
[8] Trpkovska, M., Soptrajanov, B., & Pejov, L. (2002). *Bull Chemists Technologists Macedonia*, *21*(2), 111.